The Journal of Physiological Sciences (2019) 69:223–233
https://doi.org/10.1007/s12576-018-0639-z

ORIGINAL PAPER

Protective effects of Brazilian propolis supplementation on capillary regression in the soleus muscle of hindlimb-unloaded rats

Masayuki Tanaka[1] · Miho Kanazashi[2] · Noriaki Maeshige[3] · Hiroyo Kondo[4] · Akihiko Ishihara[5] · Hidemi Fujino[3]

Received: 28 May 2018 / Accepted: 7 September 2018 / Published online: 19 September 2018

Abstract

The protective effects of Brazilian propolis on capillary regression induced by chronically neuromuscular inactivity were investigated in rat soleus muscle. Four groups of male Wistar rat were used in this study; control (CON), control plus Brazilian propolis supplementation (CON + PP), 2-week hindlimb unloading (HU), and 2-week hindlimb unloading plus Brazilian propolis supplementation (HU + PP). The rats in the CON + PP and HU + PP groups received two oral doses of 500 mg/kg Brazilian propolis daily (total daily dose 1000 mg/kg) for 2 weeks. Unloading resulted in a decrease in capillary number, luminal diameter, and capillary volume, and an increase in the expression of anti-angiogenic factors, such as p53 and TSP-1, within the soleus muscle. Brazilian propolis supplementation, however, prevented these changes in capillary structure due to unloading through the stimulation of pro-angiogenic factors and suppression of anti-angiogenic factors. These results suggest that Brazilian propolis is a potential non-drug therapeutic agent against capillary regression induced by chronic unloading.

Keywords Muscle atrophy · Capillary regression · Oxidative stress · Brazilian propolis · Hindlimb unloading · Anti-angiogenic factors

Introduction

The capillary network in skeletal muscle changes in response to physiological or pathological conditions. An increase in muscle activity, such as exercise [1, 2], and electrical stimulation [3] contribute to angiogenesis, while a decrease in neuromuscular activity, such as muscle unloading [4–7] and cast immobilization [8], and some diseases, such as cancer cachexia [9] and diabetes [10–12], leads to capillary regression.

Hindlimb unloading (HU) is a well-established rodent model of hypokinesia and hypodynamia [13] and results in capillary regression, especially within a muscle having a high percentage of slow oxidative fibers, such as the rat soleus muscle [4–7]. Various authors have reported that HU induces a decrease in the size and number of capillaries within the unloaded soleus muscle [14, 15]. These alterations have been attributed to a loss of endothelial cells due to apoptosis [7].

A chronic decrease in neuromuscular activity induces oxidative stress within the unloaded skeletal muscle. Oxidative stress has been reported to play a role in the upregulation of negative angiogenic regulators, such as thrombospondin-1 (TSP-1). Anti-angiogenic TSP-1 acts as angiogenic inhibitor through its anti-proliferative and pro-apoptotic effects [16–19]. The essential role of TSP-1 in capillary regression has been reviewed by Olfert et al. [20]. TSP-1 is also a key participant in capillary regression within the rat soleus muscle induced by HU [4]. Muscle capillarity is tuned by pro-angiogenic signaling, such as vascular endothelial

✉ Hidemi Fujino
fujino@phoenix.kobe-u.ac.jp

1 Department of Physical Therapy, Faculty of Human Sciences, Osaka University of Human Sciences, 1-4-1 Shojaku, Settsu, Osaka 566-8501, Japan

2 Department of Physical Therapy, Faculty of Health and Welfare, Prefectural University of Hiroshima, 1-1 Gakuen-cho, Mihara, Hiroshima 723-0053, Japan

3 Department of Rehabilitation Science, Kobe University Graduate School of Health Sciences, 7-10-2 Tomogaoka, Suma-ku, Kobe, Hyogo 654-0142, Japan

4 Department of Food Science and Nutrition, Nagoya Women's University, Nagoya, 4-21 Shioji-cho, Mizuho-ku, Nagoya, Aichi 467-8611, Japan

5 Laboratory of Cell Biology and Life Science, Graduate School of Human and Environmental Studies, Kyoto University, Yoshida-nihonmatsu-cho, Sakyo-ku, Kyoto, Kyoto 606-8501, Japan

growth factor (VEGF). Pro-angiogenic VEGF plays a role in angiogenesis, stimulating the formation of new vascular networks by recruiting and promoting the differentiation of endothelial cells [21]. Additionally, under the condition of muscle unloading, increased VEGF has a positive effect on angio-protection within the skeletal muscle [5, 15]. Taken together, these data suggest that pro- and anti-angiogenic factors are associated with the protection or progression of capillary regression observed in unloaded skeletal muscle.

In earlier studies, we found that supplementation with an antioxidant was an effective strategy to prevent capillary regression within unloaded muscle, with the effect achieved through modulation of the imbalance between pro- and anti-angiogenic factors [5, 6, 22]. Propolis, a substance produced by bees from the resin collected from trees and shrubs, has long been used as a non-drug therapeutic agent. It has various physiological and pathological properties, such as antivirus, antibacterial, antitumorigenesis, and antioxidant effects [23]. Brazilian propolis contains flavonoids and cinnamic acid derivatives, both of which have been revealed to possess powerful antioxidant effects [24–26]. Therefore, we hypothesized that the administration of Brazilian propolis to hindlimb unloaded rats would attenuate oxidative stress within the unloaded muscle, resulting in protection of the associated capillary regression associated with muscle atrophy. The aim of this study was to investigate the effects of propolis supplementation on capillary regression within the soleus muscle of the hindlimb-unloaded rat.

Materials and methods

Experimental design

Twenty-eight adult male Wistar rats (age 13 weeks; Japan SLC, Hamamatsu, Japan) weighing between 250 and 300 g were randomly divided into four groups: (1) control (CON), (2) control plus propolis supplementation (CON + PP), (3) hindlimb unloading (HU), and (4) hindlimb unloading plus propolis supplementation (HU + PP). HU in the rats in the HU and HU + PP groups was obtained by tail suspension for 2 weeks, as previously described [13]. Briefly, after a string was fixed to the tail with tape, a swivel hook was placed through the string just distal to the tip of the tail. The hindquarters were suspended by the tail just high enough to prevent any weight bearing of the hindlimbs on the floor of the cage. The forelimbs were allowed to maintain contact with the floor of the cage, and the suspended rats had access to water and food ad libitum. All rats were housed individually in an isolated chamber maintained at room temperature (22 ± 2 °C) under a 12:12-h light–dark cycle. This study was approved by the Institution Animal Care and Use Committee and adhered to the Kobe University Animal Experimentation Regulations (Kobe, Japan). All experimental and animal care procedures were conducted in accordance with the National Institutes of Health Guide for the Care and Use of Laboratory Animals (National Research Council, Washington DC; 1996).

Propolis supplementation

Brazilian propolis (Yamada Bee Farm, Okayama, Japan) diluted by 5% arabic gum-containing solution was administered orally by a feeding needle twice a day (500 mg/kg, with a 6-h interval between the two supplements; total daily dose 1000 mg/kg) for 2 weeks to the rats in the CON + PP and HU + PP groups. The rats in the CON and HU groups were treated similarly with a 5% arabic gum-containing solution without propolis. The non-toxicity of diet supplementation with 1000 mg/kg/day of Brazilian propolis had been confirmed in a preliminary 28-day toxicity test performed by the supplier (Yamada Bee Farm), thereby supporting our use of this dose to study disuse-induced capillary regression.

Muscle preparation

At the end of the experimental period, the rats were anaesthetized deeply by inhalation of 2% isoflurane gas via an anesthetic mask. For the histological and biological measurements, the left soleus muscle was removed and excess fat and connective tissue cleaned off, following which it was weighed, mounted on cork, and rapidly frozen in dry ice-cooled acetone. To visualize the three-dimensional capillary architecture of the soleus muscle, we examined the right soleus muscle using a confocal laser scanning method as described previously [7, 27, 28]. Briefly, a catheter was inserted into the right iliac artery, and 0.9% physiological saline containing heparin (1000 IU/l) at 37 °C was injected to wash out the intravascular blood and induce maximal vasodilation. A contrast medium (8% gelatin solution containing 1% fluorescent material) was then injected. After reflux with 50 ml of a contrast medium, the right ankle joint was held in a maximum plantar-flexion position and the entire right hindlimb was quickly immersed into ice-cooled saline. After 15 minutes, the right soleus muscle was removed and excess fat and connective tissue cleaned off; the right soleus muscle was then mounted on cork, and rapidly frozen in dry ice-cooled acetone, as described for the left soleus muscle. All frozen samples were stored at − 80 °C until subsequent analyses.

Histological analyses

The mid-belly of the left soleus muscle was mounted onto a specimen chuck using Tissue-Tek OCT compound (Sakura Finetechnical, Tokyo, Japan), and transverse

sections (thickness 12 μm) were cut on a cryostat microtome (CM3050S; Leica Microsystems, Heidelberg, Germany).

The transverse sections were stained for alkaline phosphatase (AP) to visualize capillaries; the sections were incubated in 5-bromo-4-chloro-3-indolyl phosphate/nitro blue tetrazolium for 45 min at 37 °C and fixed with 4% paraformaldehyde. The capillary-to-fiber (C/F) ratio was determined by counting capillaries and myofibers on each cryosection using microscopic images of AP staining.

In situ detection of reactive oxygen species (ROS) generation was evaluated with the fluorescent probe dihydroethidium (DHE) which detects oxidative stress by emitting light following its interaction with O_2^- to form oxyethidium. DHE is cell permeable and interacts with nucleic acids to emit a light-red color that is detectable qualitatively by fluorescent microscopy (model BX51; Olympus, Tokyo, Japan). This staining method in skeletal muscle tissues has been applied in previous studies [5, 22]. Briefly, the transverse sections (thickness 10 μm) were incubated with 5×10^{-6} mol/l DHE (Wako Pure Chemicals, Osaka, Japan) for 30 min at 37 °C in the dark box, following which the sections were rinsed with phosphate-buffered saline (PBS; 37 °C) and observed under a fluorescent microscope equipped with a filter (excitation at 545 nm). The fluorescence intensity was determined by the fluorescence area fraction using gray scale analysis in five images per muscle. All measurements were performed using Image J software program (National Institutes of Health [NIH], Bethesda, MD, USA).

Immunohistochemical staining and terminal deoxynucleotidyl transferase-mediated dUTP nick-end labeling in situ labeling

The sections (thickness 10 μm) were fixed in 4% paraformaldehyde for 10 min and blocked in 3% bovine serum albumin in PBS and 3% hydrogen peroxide in methanol for 30 min at 37 °C. They were then washed twice for 10 min in PBS, followed by incubation with dystrophin polyclonal antibody (1:400 dilution; Genentech, San Francisco, CA, USA) for 1 h at room temperature, then by incubation with DyLight 488-coupled secondary antibody (1:1000 dilution; Jackson, West Grove, PA, USA). The sections were viewed under a fluorescence microscope (model BX51; Olympus), and the fiber cross-sectional area in the left soleus muscle was determined. Terminal deoxynucleotidyl transferase-mediated dUTP nick-end labeling (TUNEL) was performed to detect apoptotic endothelial cells within the soleus muscle using in situ apoptosis detection kit (Takara, Tokyo, Japan). The sections (thickness 10 μm) were immunohistochemically stained for cluster of differentiation 31 (CD31) monoclonal antibody (1:400 dilution; Genentech, San Francisco, CA, USA) using the same procedure described above to identify endothelial cells. In the reaction with DyLight 549-coupled secondary antibody (1:1000 dilution; Jackson, West Grove, PA, USA) for CD31, the TUNEL regent was also incubated as described in the manufacturer's instructions. The stained sections were examined by fluorescence microscopy. The number of TUNEL-positive endothelial cells (yellow) was determined on each section of the soleus muscle.

Three-dimensional architecture of the capillary network

The capillary volume and luminal diameter within the right soleus muscle were determined by confocal laser scanning microscopy (model TCS-SP; Leica Microsystems) with an argon laser (488 nm). This three-dimensional (3D) imaging was performed as previously described [7, 12, 15, 27]. Briefly, the longitudinal 100-μm-thick sections were scanned to a depth of 50 μm at a slice thickness of 1 μm. Stacking in 50-slice file was converted into digital images in order to visualize the 3D architecture of the capillary network. Finally, the capillary volume ($\times 10^{-2}$ mm^3/mm^3) was measured in a 3D image (250 × 250 × 50 μm, length × width × depth), and the capillary luminal diameter (μm) was measured using the Image J software program (NIH, Bethesda, MD, USA).

Western blot analysis

A portion (approx. 20 mg) of each left soleus muscle was homogenized in RIPA lysis buffer containing 1 mM Na_3VO_4, 1 mM NaF, and protease inhibitor cocktail (1:100; P8340; Sigma-Aldrich, St. Louis, MO, USA). The total protein concentration of the supernatants was determined according to Bradford [29] using the protein assay kit of Bio-Rad Laboratories (Hercules, CA, USA). The proteins were loaded (20 μg/lane) and separated on a 12.5% sodium dodecyl sulfate–polyacrylamide gel, then blotted onto polyvinylidene difluoride membranes, and blocked for 1 h with 5% skimmed milk in PBS with Tween 20 (PBST). The membranes were incubated using antibodies against superoxide dismutase 1 (SOD-1; 1:200 in PBST; catalog no. sc-8637, Santa Cruz Biotechnology, Dallas, TX, USA), VEGF (1:200 in PBST; catalog no. sc-7269, Santa Cruz Biotechnology), or p53 (1:200 in PBST; catalog nu. sc-98; Santa Cruz Biotechnology) overnight at 4 °C, then incubated in a solution with horseradish peroxidase (HRP)-conjugated anti-goat (1:10000 in PBST) or HRP-conjugated anti-mouse (1:10000 in PBST) for 1 h. The proteins were detected using the EZWestLumi one enhanced chemiluminescence solution (ATTO, Tokyo, Japan). Finally, images were analyzed with the LAS-1000 (Fujifilm, Tokyo, Japan) chemiluminescent image analyzer and quantified using the Multi-Gauge Image Analysis Software program (Fujifilm) against the relative concentration of β-actin (1:1000 in PBST; catalog no. sc-47778; Santa Cruz Biotechnology) as an internal control.

Quantitative PCR analysis

Total RNA was extracted from approximately 10 mg of each left soleus muscle using an extraction kit (QuickGene RNA tissue kit SII; Fujifilm). Reverse transcription was carried out using the high-capacity cDNA archive kit (Applied Biosystems, Foster City, CA, USA), and cDNA samples were stored at − 20 °C until use. Expression levels of TSP-1 (Rn01513693_m1) were quantified by TaqMan Gene Expression Assays (Applied Biosystems). Each TaqMan probe and primer set was validated by performing a quantitative real-time PCR with a series of cDNA template dilutions to obtain standard curves of threshold cycle time against relative concentration using the housekeeping gene 18S as an internal standard. All samples and non-template control reactions were performed in a 7500 Fast Sequence Detection System (Applied Biosystems).

Statistical analysis

All values are expressed as mean ± standard error of the mean. Overall significant differences between the four experimental groups were determined using one-way analysis of variance followed by Tukey post hoc tests to determine specific group differences. Statistical significance was set at $P < 0.05$.

Results

Body and soleus muscle weight and muscle fiber cross-sectional areas

Absolute body weight was significantly lower in the HU and HU + PP groups than in the CON and CON + PP groups; similarly, both absolute and relative soleus muscle weight were significantly lower in the HU and HU + PP groups than in the CON and CON + PP groups. In addition, the relative muscle-to-body weight in the HU + PP group was significantly higher than that in the HU group (Table 1). The fiber cross-sectional area (FCSA) of soleus muscle was significantly decreased in the HU and HU + PP groups compared to the CON and CON + PP groups. There was no significant difference in FCSA between the HU and HU + PP groups (Table 1).

The C/F ratio

The representative images of soleus muscle stained for AP are shown for each group in Fig. 1a–d. The C/F ratios in the HU and HU + PP groups were significantly lower than those in the CON and CON + PP groups (Fig. 1e). However, the C/F ratio in the HU + PP group was significantly higher than that in the HU group (Fig. 1e).

Capillary volume and luminal diameter

The representative confocal laser scanning microscopic images of 3D capillary architecture in each group are shown in Fig. 2a–d. The capillary network in the longitudinal section of the soleus muscle appeared to be less complex in the HU group (Fig. 2c) than in the CON (Fig. 2a), CON + PP (Fig. 2b), and HU + PP (Fig. 2d) groups. The mean capillary diameter and volume in the HU group were significantly lower than those in the CON, CON + PP, and HU + PP groups (Fig. 2e, f).

The frequency distribution of capillary luminal diameter in the HU (Fig. 3c) group was shifted towards capillaries of smaller diameter compared with the CON (Fig. 3a), CON + PP (Fig. 3b), and HU + PP (Fig. 3d) groups. The percentage of capillaries with a diameter of < 2.5 μm, through which red blood cells can pass [30], increased to a high value in the HU group (17.5%) compared with the other groups (CON 4.3%, CON + PP 3.9%, HU + PP 4.9%; Fig. 3a–d).

Table 1 Body weight, soleus muscle weight, and fiber cross-sectional area

Study groups[a]	Body weight (g)	Soleus muscle absolute weight (mg)	Soleus muscle weight/body weight (mg/100 g)	Fiber cross-sectional area (μm^2)
CON	295 ± 3	116 ± 2	39.4 ± 0.9	3,029 ± 159
CON + PP	288 ± 1	115 ± 2	39.7 ± 0.9	3,242 ± 54
HU	256 ± 5*†	56 ± 2*†	21.9 ± 0.4*†	1,226 ± 44*†
HU + PP	253 ± 4*†	62 ± 1*†	24.5 ± 0.5*†‡	1,427 ± 53*†

Values in table shown as the mean ± standard error of the mean (SEM)

*, †, and ‡ indicate a significant difference from the CON, CON + PP, and HU groups, respectively, at $P < 0.05$

[a]*CON* Control group, *CON + PP* control plus propolis supplementation group, *HU* hindlimb unloading group, *HU + PP* hindlimb unloading plus propolis supplementation group

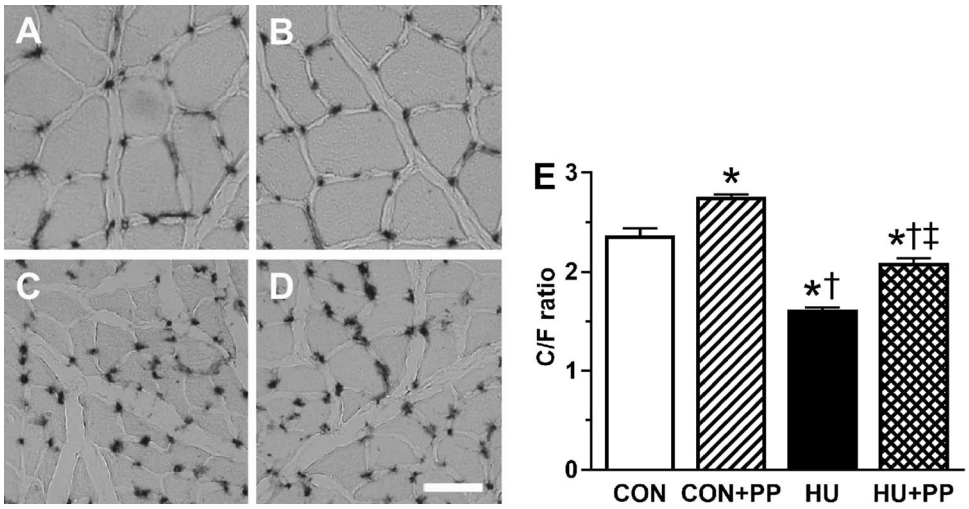

Fig. 1 Transverse sections from each group (**a** CON, **b** CON + PP, **c** HU, **d** HU + PP) stained for alkaline phosphatase (*AP*). **e** The capillary-to muscle fiber (*C/F*) ratio of the soleus muscle. *CON* Control group, *CON + PP* control plus propolis supplementation group, *HU* hindlimb unloading group, *HU + PP* hindlimb unloading plus propolis supplementation group. Scale bar: 100 μm. Values are shown as the mean (bars) ± standard deviation of the mean (SEM; error bars). The asterisk (*), dagger (†), and double dagger (‡) indicate a significant difference from the CON, CON + PP, and HU groups, respectively, at $P < 0.05$

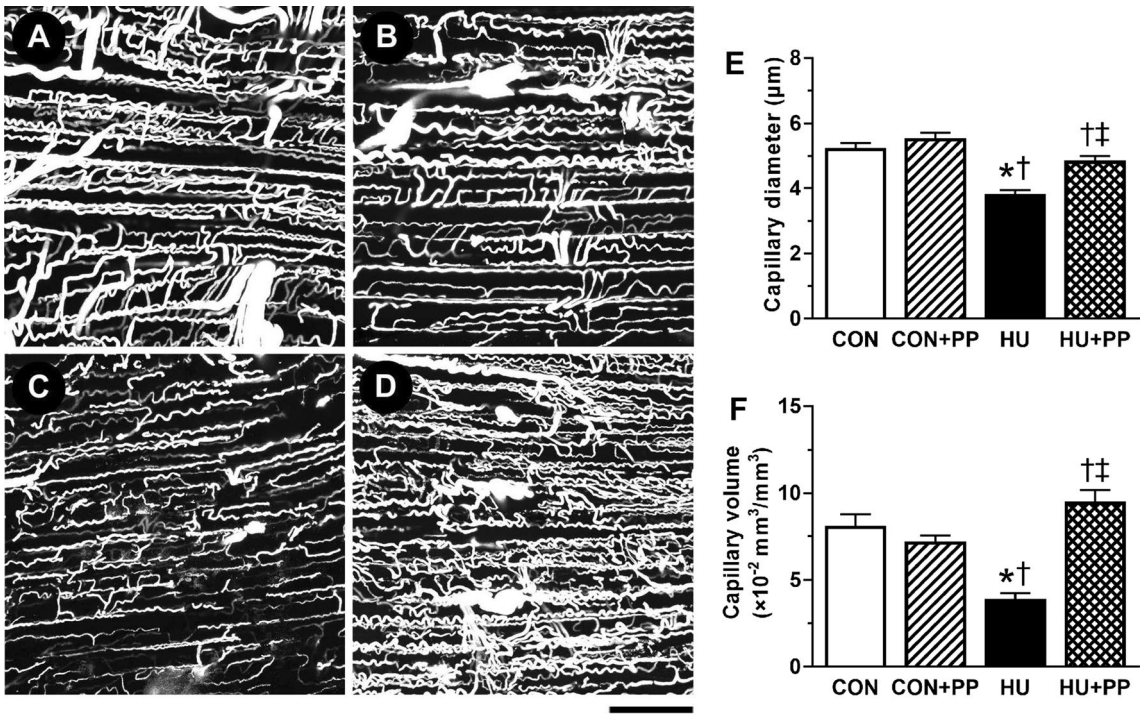

Fig. 2 Representative confocal laser scanning microscopic images of the three-dimensional (3D) capillary architecture of the soleus muscle of a rat in the CON (**a**), CON + PP (**b**), HU (**c**), and HU + PP (**d**) groups. Scale bar: 100 μm. **e**, **f** Mean capillary luminal diameter (**e**) and capillary volume (**f**) in the soleus muscle of each group. Values are shown as the mean (bars) ± SEM (error bars). The asterisk (*), dagger (†), and double dagger (‡) indicate a significant difference from the CON, CON + PP, and HU groups, respectively, at $P < 0.05$

ROS production and SOD-1 protein levels

Intracellular ROS production was measured by DHE fluorescence in the nucleus. The representative images of the soleus muscle stained with DHE in each group are shown in Fig. 4a–d. DHE fluorescence in the HU group

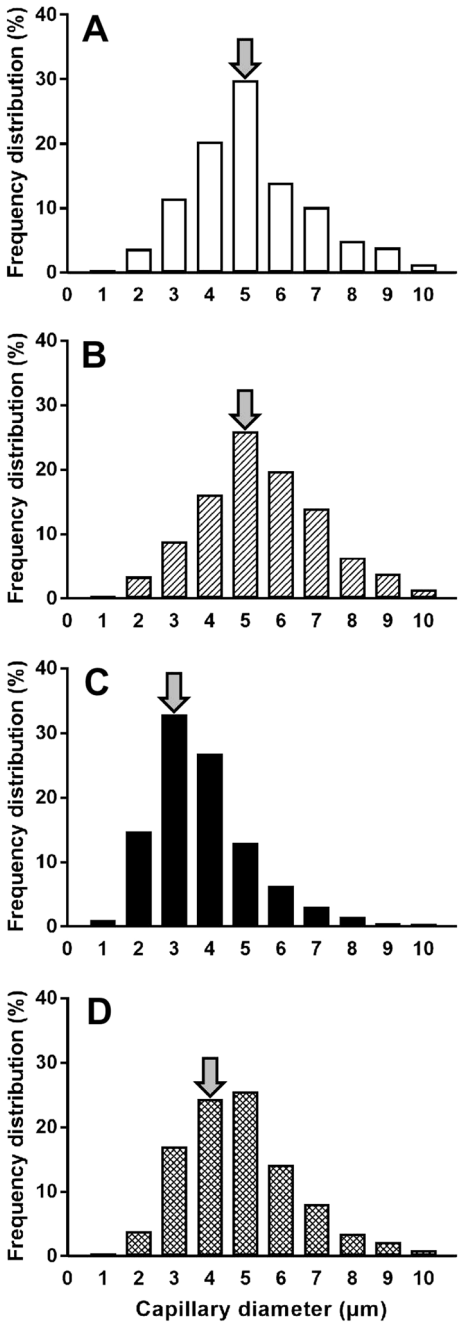

Fig. 3 Frequency distribution of capillary luminal diameter in the CON (**a**), CON + PP (**b**), HU (**c**), and HU + PP (**d**) groups. Arrows indicate the median of capillary diameter

was significantly higher than that in the CON, CON + PP, and HU + PP groups (Fig. 4e). The value in the HU + PP group was consistently similar to that in the CON and CON + PP group.

The protein level of the primary cellular enzymatic antioxidant SOD-1 was determined by western blotting. The expression level of SOD-1 protein was significantly higher in the HU group than in the CON, CON + PP, and HU + PP groups, whereas the level in the HU + PP group did not differ from that in the CON and CON + PP groups (Fig. 4f).

Protein expression level of p53 and mRNA expression level of TSP-1

The protein expression level of p53, one of anti-angiogenic factors, was significantly increased in the HU group compared with the CON group, while the value in the HU + PP group was maintained at the CON level (Fig. 5a). Similarly, the mRNA expression level of TSP-1, one of the anti-angiogenic factors tested, was significantly increased in the HU group compared with the other groups, while the expression level in the HU + PP group was maintained at the CON level (Fig. 5b).

Protein expression level of VEGF

The expression level of VEGF protein, one of the pro-angiogenic factors tested, in the HU group did not differ from that in the CON group. However, the level in the HU + PP group was significantly higher than that in the HU group (Fig. 6).

Apoptosis of endothelial cells

Apoptosis of endothelial cells was identified by staining with TUNEL and CD-31 on transverse section of soleus muscle. The representative images of TUNEL-positive endothelial cells were shown in the Fig. 7a–c. The frequency of TUNEL-positive endothelial cells in the HU group was significantly higher than that in the CON, CON + PP, and HU + PP groups, and the value in the HU + PP was maintained at the CON level (Fig. 7d).

Discussion

The novel findings of this study are that the administration of Brazilian propolis prevented both overexpression of ROS due to a chronic decrease in neuromuscular activity and capillary regression by suppressing anti-angiogenic signaling and stimulating pro-angiogenic signaling within the atrophied soleus muscle. Based on these results, we suggest that Brazilian propolis treatment is an effective therapy for capillary regression in the chronically unloaded skeletal muscle.

The capillary network in skeletal muscle is susceptible to structural changes in response to various conditions. Previous studies have reported that neuromuscular inactivity results in not only a reduction of capillary number [4, 14], but also a decrease in capillary luminal diameter and volume within the unloaded soleus muscle [5, 7, 15]. Additionally, capillaries with a diameter < 2.5 μm, through which erythrocytes can pass [30], were observed more frequently

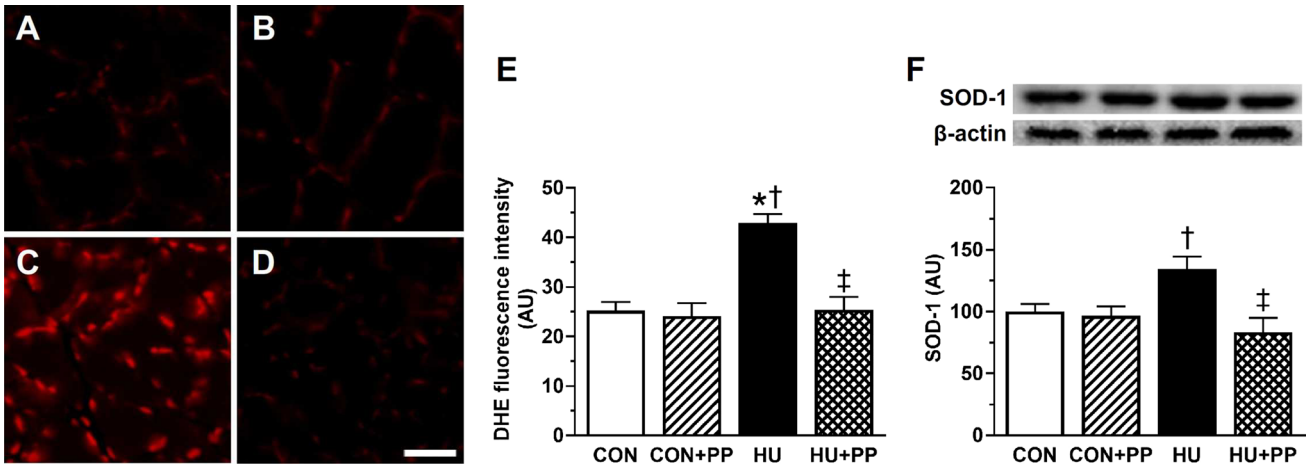

Fig. 4 Transverse sections from each group (**a** CON, **b** CON + PP, **c** HU, **d** HU + PP) stained with the fluorescent probe dihydroethidium (*DHE*) that detects oxidative stress. **e**, **f** Mean levels of DHE fluorescence (**e**) and superoxide dismutase 1 (*SOD-1*) protein expression (**f**) in the soleus muscle of each group. Scale bar: 50 µm. Values are shown as the mean (bars) ± SEM (error bars). The asterisk (*), dagger (†), and double dagger (‡) indicate a significant difference from the CON, CON + PP, and HU groups, respectively, at $P < 0.05$. *AU* Arbitrary units

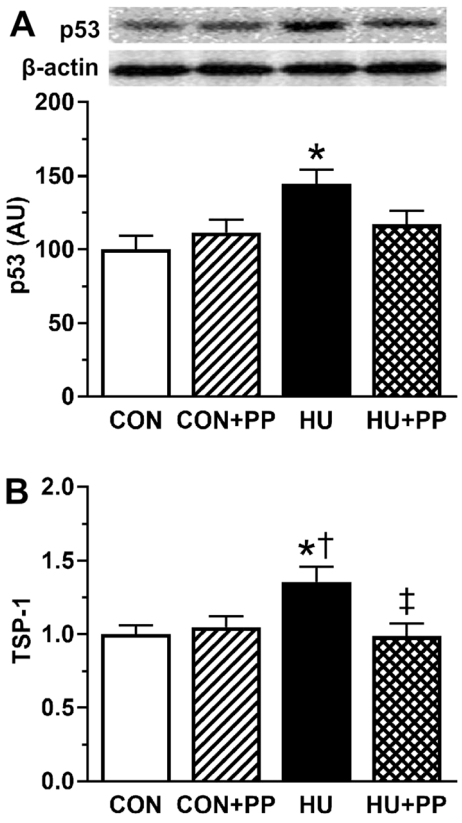

Fig. 5 Mean levels of p53 protein expression (**a**) and mean levels of thrombospondin-1 (*TSP-1*) mRNA (**b**) in the soleus muscles of each group. Values are shown as the mean (bars) ± SEM (error bars). The asterisk (*), dagger (†), and double dagger (‡) indicate a significant difference from the CON, CON + PP, and HU groups, respectively, at $P < 0.05$

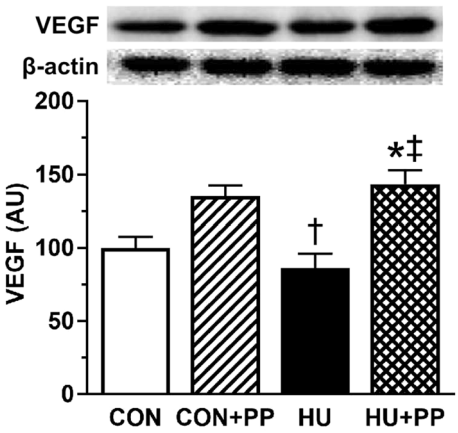

Fig. 6 Mean levels of vascular endothelial growth factor (*VEGF*) protein expression in the soleus muscles of each group. Values are shown as the mean (bars) ± SEM (error bars). The asterisk (*), dagger (†), and double dagger (‡) indicate a significant difference from the CON, CON + PP, and HU groups, respectively, at $P < 0.05$

in unloaded skeletal muscle than in the skeletal muscle of grounded rats. This result indicates that unloading increases dysfunctional capillaries within the skeletal muscle. Taken together, these results are consistent with those observed in the present study.

Oxidative stress is increased within an unloaded muscle due to an overproduction of ROS [31–33]. Additionally, oxidative stress associated with unloading has been shown to participate in the pathophysiology of capillary regression within the skeletal muscle, as shown in studies using antioxidant treatment [5, 22]. Therefore, we also investigated oxidative stress in the present study. As a marker for

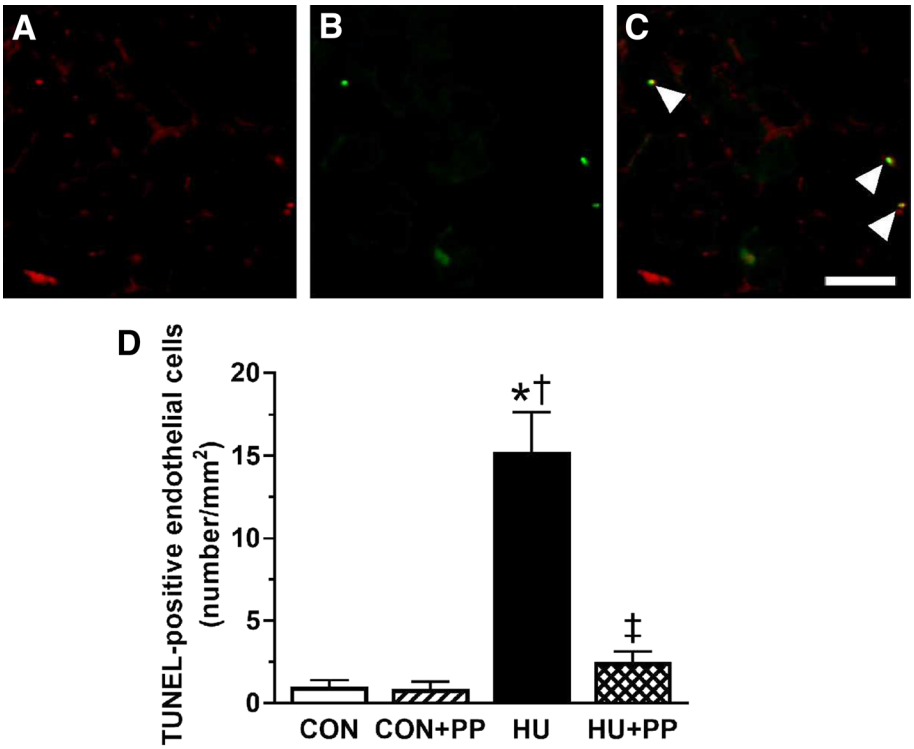

Fig. 7 Microscopic images of the soleus muscle stained with cluster of differentiation 31 (CD31; **a**) and terminal deoxynucleotidyl transferase-mediated dUTP nick-end labeling (*TUNEL*; **b**); **c** merged images of **a** and **b**. Scale bar: 50 µm. Arrowheads indicate TUNEL-positive endothelial cells. **d** Mean number of the TUNEL-positive endothelial cells of the soleus muscle in each group. Values are shown as the mean (bars) ± SEM (error bars). The asterisk (*), dagger (†), and double dagger (‡) indicate a significant difference from the CON, CON + PP, and HU groups, respectively, at $P < 0.05$

oxidative stress, we examined DHE fluorescence intensity and SOD-1 protein expression within the unloaded soleus muscle [5, 22, 34]. Our results show that HU enhanced both DHE fluorescence intensity and SOD-1 protein expression, thereby reflecting increased oxidative stress within the unloaded soleus muscle, which is consistent with the findings of earlier studies [5, 22, 34]. Oxidative stress increases protein expression of transcriptional factor p53 [35], known as a tumor suppressor protein [36]. p53 plays a key role in regulating various signaling pathways to maintain skeletal muscle health [37]. It has been reported that the increase in p53 protein expression induces endothelial cell apoptosis and then suppresses angiogenesis [38, 39]. Indeed, p53 protein expression has been found to increase within the unloaded soleus muscle [40]. Roudier et al. demonstrated that HU-related p53 protein expression participates in capillary regression by upregulating TSP-1 protein expression [4], leading to endothelial cell apoptosis. However, Roudier et al. also reported that p53 does not play a role in the decreased VEGF protein expression in response to unloading [4]. The results of our present study on the expression of these proteins are consistent with those reported by Roudier et al. [4]. In addition, in a review of the literature, Olfert et al. found that capillary regression depends on increasing TSP-1 expression but not on decreasing VEGF expression [20]. Our present results clearly suggest that HU-induced oxidative stress leads to capillary regression via the upregulation of p53 and its downstream TSP-1 expression, with support provided by our observation of increased endothelial cell apoptosis, as expressed in TUNEL-positive endothelial cells within the unloaded soleus muscle.

Antioxidants can be regarded as countermeasures for disuse-induced microangiopathy. Results from earlier studies suggest that supplementation with anti-oxidative food components could attenuate disuse-induced capillary regression [5, 22]. Brazilian propolis contains a variety of bioactive components and possesses many biological and pharmacological properties [23], and it has been used since ancient times as a non-drug therapeutic agent. Brazilian propolis also has antioxidant activity due to its content of flavonoids [24] and cinnamic acid derivatives [25, 26]. Our study of the effects of Brazilian propolis on unloading-induced oxidative stress revealed that Brazilian propolis suppressed the ROS production observed in DHE fluorescence intensity and SOD-1 protein expression studies within the unloaded soleus muscle to near control levels. These results suggest that Brazilian propolis bestows protective effects on unloading-induced oxidative stress within the muscle. We also found that Brazilian propolis attenuated the unloading-induced changes in anti-angiogenic factors and capillary architecture within the skeletal muscle. These results are in agreement with those reported in our previous studies [5, 22] in which we used the powerful antioxidant astaxanthin, leading use to presume that Brazilian propolis administered daily into

disused muscle exhibits antioxidant and resultant vascular protective effects equivalent to those with daily antioxidant astaxanthin supplementation. Antioxidant treatment has been found to attenuate the p53-related anti-angiogenic pathway through scavenging ROS [41, 42]. Some of the components of Brazilian propolis have been reported to be associated with angio-protective effects via modulation of oxidative stress [43, 44]. Therefore, the prevention of capillary regression by Brazilian propolis observed in the study can likely be explained by the regulation of oxidative stress and related negative angiogenic regulators, such as p53 and TSP-1. This notion is supported by the observation of the suppression of endothelial cell apoptosis within the unloaded muscle treated with Brazilian propolis.

We observed an increase in VEGF protein expression within the unloaded muscle treated with Brazilian propolis. Decreased VEGF expression may have little involvement in capillary regression [20], but increased VEGF expression prevents unloading-induced capillary regression [15, 22]. Thus, Brazilian propolis may prevent capillary regression by increasing pro-angiogenic VEGF protein expression, which is a novel effect of Brazilian propolis. However, further investigations are needed to clarify the underlying mechanism in Brazilian propolis-related VEGF protein expression observed in the present study.

Anti-tumorigenic effects of Brazilian propolis have been demonstrated in various cancers in both animal and in vitro models [45–47]. The anti-tumorigenic effect can be explained mainly by the pro-apoptotic [48] and anti-angiogenic activities [49] of the active components in Brazilian propolis. In the present study, however, we found that Brazilian propolis did not induce endothelial cell apoptosis or capillary regression within the soleus muscle of rats treated with or without HU, which seems to suggest a role for endothelial cytoprotection in skeletal muscle. These results may indicate that Brazilian propolis exerts both pro- and anti-apoptotic effects depending on cellular status. Additionally, an in vitro toxicological study of Brazilian propolis by Xuan et al. showed that a high concentration of Brazilian propolis increases ROS production and p53-dependent apoptosis in human umbilical vein endothelial cells but that a low concentration decreases both processes [50]. This result means that Brazilian propolis has both pro-cytotoxic and anti-cytotoxic activity depending on its concentration. In our study, we administered a daily oral dose of Brazilian propolis of 1000 mg/kg to rats for 2 weeks; the safety of this dose in terms of toxicity and frequency of administration had been confirmed in preliminary in vivo experiments by the manufacturer. Therefore, our results support the possibility that Brazilian propolis acts as an anti-cytotoxic agent within the soleus muscle. However, we did not investigate the dose-dependent effects of Brazilian propolis on capillary regression in disused muscle. Further studies are needed to clarify this issue.

In conclusion, the results of our study indicate for the first time that the administration of Brazilian propolis has protective effects on the capillary regression that accompanies chronic muscle unloading. The angio-protective effects of Brazilian propolis may be attributed its bioactive components which lead to a suppression of the anti-angiogenic pathway and stimulation of the pro-angiogenic pathway. Therefore, Brazilian propolis seems to be a non-drug therapeutic agent that is applicable to the treatment of skeletal muscular angiopathy that occurs in various situations, such as bed rest, cast immobilization, diabetes, and cancer cachexia.

Conclusion

In conclusion, we found that Brazilian propolis supplementation was an effective treatment to attenuate capillary regression in soleus muscle associated with prolonged mechanical unloading. Our results suggest that Brazilian propolis can be administered as a therapeutic intervention for the treatment of skeletal muscle angiopathy due to disuse-induced muscle atrophy.

Acknowledgements This study was supported by Grants-in-Aid for Scientific Research (No. 16H07361, No. 16K12732, and No. 15K16516) from Japanese Ministry of Education, Culture, Sports, science and Technology, and Yamada Research Grant. The funding agency had no role in the study design, data collection, and analysis, decision to publish, or preparation of the manuscript.

Author contributions MT, MK, and HF conceived and designed the experiments. MT and MK performed the experiments. MT, MK, and HF analyzed the data. MK, NM, HK, AI, and HF contributed by providing regents, materials and analysis tools. MT, HK, AI, and HF interpreted the data and wrote the paper. All authors approved the final version of the manuscript.

Funding This study was supported by Grants-in-Aid for Scientific Research (No. 16H07361, No. 16K12732, and No. 15K16516) from Japanese Ministry of Education, Culture, Sports, science and Technology, and Yamada Research Grant.

Compliance with ethical standards

Conflict of interest The authors declare that they have no conflict of interest.

Ethical approval All applicable international, national, and/or institutional guidelines for the care and use of animals were followed. All procedures performed in studies involving animals were in accordance with the ethical standards of the institution or practice at which the studies were conducted. This article does not contain any studies with human participants performed by any of the authors.

References

1. Slopack D, Roudier E, Liu ST, Nwadozi E, Birot O, Haas TL (2014) Forkhead BoxO transcription factors restrain exercise-induced angiogenesis. J Physiol 592:4069–4082
2. Delavar H, Nogueira L, Wagner PD, Hogan MC, Metzger D, Breen EC (2014) Skeletal myofiber VEGF is essential for the exercise training response in adult mice. Am J Physiol Regul Integr Comp Physiol 306:R586–R595
3. de Leon EB, Bortoluzzi A, Rucatti A, Nunes RB, Saur L, Rodrigues M, Oliveira U, Alves-Wagner AB, Xavier LL, Machado UF, Schaan BD, Dall'Ago P (2011) Neuromuscular electrical stimulation improves GLUT-4 and morphological characteristics of skeletal muscle in rats with heart failure. Acta Physiol (Oxf) 201:265–273
4. Roudier E, Gineste C, Wazna A, Dehghan K, Desplanches D, Birot O (2010) Angio-adaptation in unloaded skeletal muscle: new insights into an early and muscle type-specific dynamic process. J Physiol 588:4579–4591
5. Kanazashi M, Tanaka M, Murakami S, Kondo H, Nagatomo F, Ishihara A, Roy RR, Fujino H (2014) Amelioration of capillary regression and atrophy of the soleus muscle in hindlimb-unloaded rats by astaxanthin supplementation and intermittent loading. Exp Physiol 99:1065–1077
6. Hirayama Y, Nakanishi R, Maeshige N, Fujino H (2017) Preventive effects of nucleoprotein supplementation combined with intermittent loading on capillary regression induced by hindlimb unloading in rat soleus muscle. Physiol Rep 5(4). https://doi.org/10.14814/phy2.13134
7. Fujino H, Kohzuki H, Takeda I, Kiyooka T, Miyasaka T, Mohri S, Shimizu J, Kajiya F (2005) Regression of capillary network in atrophied soleus muscle induced by hindlimb unweighting. J Appl Physiol 98:1407–1413
8. Qin L, Appell HJ, Chan KM, Maffulli N (1997) Electrical stimulation prevents immobilization atrophy in skeletal muscle of rabbits. Arch Phys Med Rehabil 78:512–517
9. Julienne CM, Dumas JF, Goupille C, Pinault M, Berri C, Collin A, Tesseraud S, Couet C, Servais S (2012) Cancer cachexia is associated with a decrease in skeletal muscle mitochondrial oxidative capacities without alteration of ATP production efficiency. J Cachexia Sarcopenia Muscle 3:265–275
10. Kivela R, Silvennoinen M, Touvra AM, Lehti TM, Kainulainen H, Vihko V (2006) Effects of experimental type 1 diabetes and exercise training on angiogenic gene expression and capillarization in skeletal muscle. FASEB J 20:1570–1572
11. Roudier E, Forn P, Perry ME, Birot O (2012) Murine double minute-2 expression is required for capillary maintenance and exercise-induced angiogenesis in skeletal muscle. FASEB J 26:4530–4539
12. Kondo H, Fujino H, Murakami S, Tanaka M, Kanazashi M, Nagatomo F, Ishihara A, Roy RR (2015) Low-intensity running exercise enhances the capillary volume and pro-angiogenic factors in the soleus muscle of type 2 diabetic rats. Muscle Nerve 51:391–399
13. Morey-Holton ER, Globus RK (1985) Hindlimb unloading rodent model: technical aspects. J Appl Physiol 92:1367–1377
14. Kano Y, Shimegi S, Takahashi H, Masuda K, Katsuta S (2000) Changes in capillary luminal diameter in rat soleus muscle after hind-limb suspension. Acta Physiol Scand 169:271–276
15. Hirayama Y, Nakanishi R, Tategaki A, Maeshige N, Kondo H, Ishihara A, Roy RR, Fujino H (2017) Enterococcus faecium strain R30 increases red blood cell velocity and prevents capillary regression in the soleus of hindlimb-unloaded rats via the eNOS/VEGF pathway. Microcirculation 24(4). https://doi.org/10.1111/micc.12356
16. Resovi A, Pinessi D, Chiorino G, Taraboletti G (2014) Current understanding of the thrombospondin-1 interactome. Matrix Biol 37:83–91
17. Primo L, Ferrandi C, Roca C, Marchio S, di Blasio L, Alessio M, Bussolino F (2005) Identification of CD36 molecular features required for its in vitro angiostatic activity. FASEB J 19:1713–1715
18. Febbraio M, Hajjar DP, Silverstein RL (2001) CD36: a class B scavenger receptor involved in angiogenesis, atherosclerosis, inflammation, and lipid metabolism. J Clin Invest 108:785–791
19. Chen H, Herndon ME, Lawler J (2000) The cell biology of thrombospondin-1. Matrix Biol 19:597–614
20. Olfert IM (2016) Physiological capillary regression is not dependent on reducing VEGF expression. Microcirculation 23:146–156
21. Olsson AK, Dimberg A, Kreuger J, Claesson-Welsh L (2006) VEGF receptor signalling—in control of vascular function. Nat Rev Mol Cell Biol 7:359–371
22. Kanazashi M, Okumura Y, Al-Nassan S, Murakami S, Kondo H, Nagatomo F, Fujita N, Ishihara A, Roy RR, Fujino H (2013) Protective effects of astaxanthin on capillary regression in atrophied soleus muscle of rats. Acta Physiol (Oxf) 207:405–415
23. Pasupuleti VR, Sammugam L, Ramesh N, Gan SH (2017) Honey, propolis, and royal jelly: a comprehensive review of their biological actions and health benefits. Oxid Med Cell Longev 2017:article ID 1259510. https://doi.org/10.1155/2017/1259510
24. Wang D, Zhang X, Li D, Hao W, Meng F, Wang B, Han J, Zheng Q (2017) Kaempferide protects against myocardial ischemia/reperfusion injury through activation of the PI3 K/Akt/GSK-3beta pathway. Mediat Inflamm 2017:5278218
25. Veiga RS, De Mendonca S, Mendes PB, Paulino N, Mimica MJ, Lagareiro Netto AA, Lira IS, Lopez BG, Negrao V, Marcucci MC (2017) Artepillin C and phenolic compounds responsible for antimicrobial and antioxidant activity of green propolis and *Baccharis dracunculifolia* DC. J Appl Microbiol 122:911–920
26. Uto Y, Ae S, Koyama D, Sakakibara M, Otomo N, Otsuki M, Nagasawa H, Kirk KL, Hori H (2006) Artepillin C isoprenomics: design and synthesis of artepillin C isoprene analogues as lipid peroxidation inhibitor having low mitochondrial toxicity. Bioorg Med Chem 14:5721–5728
27. Fujino H, Kondo H, Murakami S, Nagatomo F, Fujita N, Takeda I, Ishihara A, Roy RR (2012) Differences in capillary architecture, hemodynamics, and angiogenic factors in rat slow and fast plantarflexor muscles. Muscle Nerve 45:242–249
28. Kondo H, Fujino H, Murakami S, Nagatomo F, Roy RR, Ishihara A (2011) Regressed three-dimensional capillary network and inhibited angiogenic factors in the soleus muscle of non-obese rats with type 2 diabetes. Nutr Metab (Lond) 8:77
29. Bradford MM (1976) A rapid and sensitive method for the quantitation of microgram quantities of protein utilizing the principle of protein-dye binding. Anal Biochem 72(1–2):248–254
30. Henquell L, LaCelle PL, Honig CR (1976) Capillary diameter in rat heart in situ: relation to erythrocyte deformability, O_2 transport, and transmural O_2 gradients. Microvasc Res 12:259–274
31. Powers SK, Kavazis AN, McClung JM (2007) Oxidative stress and disuse muscle atrophy. J Appl Physiol 102:2389–2397
32. Yoshihara T, Yamamoto Y, Shibaguchi T, Miyaji N, Kakigi R, Naito H, Goto K, Ohmori D, Yoshioka T, Sugiura T (2017) Dietary astaxanthin supplementation attenuates disuse-induced muscle atrophy and myonuclear apoptosis in the rat soleus muscle. J Physiol Sci 67:181–190
33. Servais S, Letexier D, Favier R, Duchamp C, Desplanches D (2007) Prevention of unloading-induced atrophy by vitamin E supplementation: links between oxidative stress and soleus muscle proteolysis? Free Radic Biol Med 42:627–635

34. Maezawa T, Tanaka M, Kanazashi M, Maeshige N, Kondo H, Ishihara A, Fujino H (2017) Astaxanthin supplementation attenuates immobilization-induced skeletal muscle fibrosis via suppression of oxidative stress. J Physiol Sci 67:603–611
35. Chen J, Goligorsky MS (2006) Premature senescence of endothelial cells: methusaleh's dilemma. Am J Physiol Heart Circ Physiol 290:H1729–H1739
36. Mello SS, Attardi LD (2017) Deciphering p53 signaling in tumor suppression. Curr Opin Cell Biol 51:65–72
37. Beyfuss K, Hood DA (2018) A systematic review of p53 regulation of oxidative stress in skeletal muscle. Redox Rep 23(1):100–117
38. Dai F, Chen Y, Song Y, Huang L, Zhai D, Dong Y, Lai L, Zhang T, Li D, Pang X, Liu M, Yi Z (2012) A natural small molecule harmine inhibits angiogenesis and suppresses tumour growth through activation of p53 in endothelial cells. PLoS One 7:e52162
39. Kruse JP, Gu W (2009) Modes of p53 regulation. Cell 137:609–622
40. Siu PM, Pistilli EE, Murlasits Z, Alway SE (2006) Hindlimb unloading increases muscle content of cytosolic but not nuclear Id2 and p53 proteins in young adult and aged rats. J Appl Physiol 100:907–916
41. Feng T, Wang L, Zhou N, Liu C, Cui J, Wu R, Jing J, Zhang S, Chen H, Wang S (2017) Salidroside, a scavenger of ROS, enhances the radioprotective effect of Ex-RAD(R) via a p53Dependent apoptotic pathway. Oncol Rep 38:3094–3102
42. Zhao H, Ma T, Fan B, Yang L, Han C, Luo J, Kong L (2016) Protective effect of trans-delta-viniferin against high glucose-induced oxidative stress in human umbilical vein endothelial cells through the SIRT1 pathway. Free Radic Res 50:68–83
43. Goutzourelas N, Stagos D, Spanidis Y, Liosi M, Apostolou A, Priftis A, Haroutounian S, Spandidos DA, Tsatsakis AM, Kouretas D (2015) Polyphenolic composition of grape stem extracts affects antioxidant activity in endothelial and muscle cells. Mol Med Rep 12:5846–5856
44. Fuentes E, Palomo I (2014) Mechanisms of endothelial cell protection by hydroxycinnamic acids. Vascul Pharmacol 63:155–161
45. Frion-Herrera Y, Diaz-Garcia A, Ruiz-Fuentes J, Rodriguez-Sanchez H, Sforcin JM (2015) Brazilian green propolis induced apoptosis in human lung cancer A549 cells through mitochondrial-mediated pathway. J Pharm Pharmacol 67:1448–1456
46. Ishihara M, Naoi K, Hashita M, Itoh Y, Suzui M (2009) Growth inhibitory activity of ethanol extracts of Chinese and Brazilian propolis in four human colon carcinoma cell lines. Oncol Rep 22:349–354
47. Szliszka E, Zydowicz G, Janoszka B, Dobosz C, Kowalczyk-Ziomek G, Krol W (2011) Ethanolic extract of Brazilian green propolis sensitizes prostate cancer cells to TRAIL-induced apoptosis. Int J Oncol 38:941–953
48. Kimoto T, Arai S, Kohguchi M, Aga M, Nomura Y, Micallef MJ, Kurimoto M, Mito K (1998) Apoptosis and suppression of tumor growth by artepillin C extracted from Brazilian propolis. Cancer Detect Prev 22:506–515
49. Ahn MR, Kunimasa K, Ohta T, Kumazawa S, Kamihira M, Kaji K, Uto Y, Hori H, Nagasawa H, Nakayama T (2007) Suppression of tumor-induced angiogenesis by Brazilian propolis: major component artepillin C inhibits in vitro tube formation and endothelial cell proliferation. Cancer Lett 252:235–243
50. Xuan H, Zhao J, Miao J, Li Y, Chu Y, Hu F (2011) Effect of Brazilian propolis on human umbilical vein endothelial cell apoptosis. Food Chem Toxicol 49:78–85